OECD/MCCI-2008-TR04

OECD MCCI Project
Category 2 Coolability Engineering Enhancement Tests:
Water-Cooled Basemat Test 1 (WCB-1) Test Plan

Rev. 2 - Final

June 2008

by:

M. T. Farmer, D. J. Kilsdonk, S. Lomperski, and R. W. Aeschlimann

Nuclear Engineering Division
Argonne National Laboratory
9700 S. Cass Avenue
Argonne, IL 60439 USA

Table of Contents

1. INTRODUCTION.....1
1.1 Background.....1
1.2 Objectives and Approach.....2

2. FACILITY DESCRIPTION.....3
2.1 Test Apparatus.....3
2.2 Instrumentation and Data Acquisition.....11
2.3 Corium Composition.....14
2.4 Concrete Composition.....14

3. TEST PROCEDURES.....16
3.1 Pretest Preparations.....16
3.2 Test Operations.....17
3.3 Posttest Procedures.....17

4. REFERENCES.....18

List of Figures

Figure **Page**

2-1 Schematic of WCB-1 Test Facility....3

2-2 Side View of Test Section Showing Water-Cooled Basemat Installation....4

2-3 Fabrication Details of Water-Cooled Basemat....6

2-4 Details of Basemat Waterline and Instrumentation Feed Throughs....6

2-5 Details of Basemat Heat Flux Meter Installation....7

2-6 Basemat Water Channel Cooling Circuit (1 of 5)....8

2-7 Test Section Water Supply System....11

2-8 Plan View of Basemat Instrumentation Layout (dimensions are in cm)....12

2-9 Elevation View of Basemat Type C Thermocouple Locations....12

2-10 WCB Data Acquisition and Control Systems....13

List of Tables

Table **Page**

1-1 Specifications for WCB-1....2

2-1 Thermophysical Properties Assumed in the Analysis....9

2-2 Channel Thermal Analysis at Design Basis Conditions....9

2-3 Post-Reaction Bulk Composition for WCB-1 Thermite....15

2-4 Detailed Pre- and Post-Reaction Compositions for WCB-1 Thermite....15

2-5 Engineering Composition of WCB-1 Siliceous Concrete Basemat....15

2-6 Chemical Composition of Siliceous Concrete (CCI-3 basis [2])....16

1.0 INTRODUCTION

1.1 Background

Ex-vessel debris coolability is an important light water reactor (LWR) safety issue. For existing plants, resolution of this issue will confirm the technical basis for severe accident management guidelines (SAMGs). For new reactors, understanding this issue will help confirm the effectiveness of the design and implementation of new accident mitigation features and severe accident management design alternatives (SAMDAs). The first OECD-MCCI program conducted reactor material experiments focused on achieving the following technical objectives: i) provide confirmatory evidence and data for various cooling mechanisms through separate effect tests for severe accident model development, and ii) provide long-term 2-D core-concrete interaction data for code assessment and improvement.

Debris cooling mechanisms investigated as part of the first MCCI program included: i) water ingression through cracks/fissures in the core debris, ii) melt eruption caused by gas sparging, and iii) large-scale crust mechanical failure leading to renewed bulk cooling. The results of this testing and associated analysis provided an envelope (principally determined by melt depth) for debris coolability. However, this envelope does not encompass the full range of potential melt depths for all plant accident sequences. Cooling augmentation by additional means may be needed at the late stage to assure coolability for new reactor designs as well as for various accident sequences for existing reactors. In addition, the results of the CCI tests showed that lateral/axial power split is a function of concrete type. However, the first program produced limited data sets for code assessment. In light of significant differences in ablation behavior for different concrete types, additional data will be useful in reducing uncertainties and gaining confidence in code predictions.

Based on these findings, a broad workscope was defined for the follow-on MCCI program. The workscope can be divided into the following four categories:

1. Combined effect tests to investigate the interplay of different cooling mechanisms, and to provide data for model development and code assessment purposes.
2. Tests to investigate new design features to enhance coolability, applicable particularly to new reactor designs.
3. Tests to generate two-dimensional core-concrete interaction data.
4. Integral tests to validate severe accident codes.

In addition to the experimental work, an analysis task was defined to develop and validate coolability models to form the basis for extrapolating the experiment findings to plant conditions.

As one of the steps required to satisfy these objectives, the Management Board (MB) approved the conduct of the first Category 2 Test. To this end, the MB convened a subcommittee at the 2nd PRG meeting to recommend testing options to investigate generic approaches for augmenting ex-vessel corium coolability in new reactors. Based on these interactions, the MB approved the following PRG recommendation at the 3rd PRG meeting regarding the first large-scale test:

The PRG recommends that a large scale test with the water surface cooled concept be performed. The PRG took note that some members raised concerns about cost. The PRG recommends that the OA refines the test design proposed at the meeting consistently with comments received, and submit the final test specifications to PRG within three months for approval within an additional six weeks.

1.2 Objectives and Approach

In response to this recommendation, the objective of this document is to provide a summary test plan for the first Water-Cooled Basemat test (WCB-1) for PRG review. Test specifications are provided in Table 1-1. The experiment approach is to incorporate a water-cooled basemat into the core-concrete interaction test apparatus. The basemat is composed of five parallel water channels that are instrumented to provide both local and global data on the heat transfer performance. The basemat is covered with a layer of sacrificial concrete that will be ablated by the overlying melt at the start of the experiment. Eventually, the melt will approach and then be thermally stabilized at the interface of the water-cooled basemat. The test is thus designed to provide prototypic data on the transient evolution and stabilization of a core melt in a generic water-cooled core catcher design for advanced plant applications.

Table 1-1. Specifications for WCB-1.

Parameter	Specification
Corium	100 % oxidized PWR with 8 wt % siliceous concrete
Test section cross-sectional area	50 cm x 50 cm
Initial melt mass (depth)	400 kg (25 cm)
Test section sidewall construction	MgO protected by UO_2 pellet layer.
Basemat construction	0-15 cm depth: siliceous concrete
	15-19.4 cm: water-cooled basemat, 5 parallel channels.
System operating pressure	Atmospheric
Melt formation technique (timescale)	Chemical reaction (~30 seconds)
Initial melt temperature	1950 ºC
Melt heating technique	Direct Electrical (Joule) Heating
Initial power input level	Constant power at 80 kW[a]
Inlet water temperature	15 ºC
Inlet water flow rate	2 liters/second
Sustained water depth over melt	50 ± 5 cm

[a]Based on 150 kW/m^2 design heat flux to bottom and top surfaces of melt (0.5 m^2 area), plus an additional 5 kW to compensate for a long-term heat losses of 10 kW/m^2 to MgO sidewalls (0.5 m^2 area).

2.0 FACILITY DESCRIPTION

The high-level experiment objective of WCB-1 is to provide reactor material test data on the transient evolution and stabilization of a core melt within a generic water-cooled core catcher design for advanced plant applications. The experiment approach is to incorporate a test section featuring a water-cooled basemat into the Core Concrete Interaction (CCI) test facility to study thermal performance under long-term conditions in which melt resistance heating is provided to simulate decay heat. Additional details regarding the proposed test design and operating procedures are provided in the balance of this section.

2.1 Test Apparatus

The WCB-1 test facility consists of a test apparatus, a power supply for Direct Electrical Heating (DEH) of the corium, a water supply system, two steam condensation (quench) tanks, a ventilation system to complete filtration and exhaust the off-gases, and a data acquisition system. A schematic illustration of the facility is provided in Figure 2-1. The apparatus consists of three rectilinear sidewall sections and a lid. The overall structure is 3.4 m tall. The sidewall sections have a square internal cross sectional area of nominally 50 cm x 50 cm.

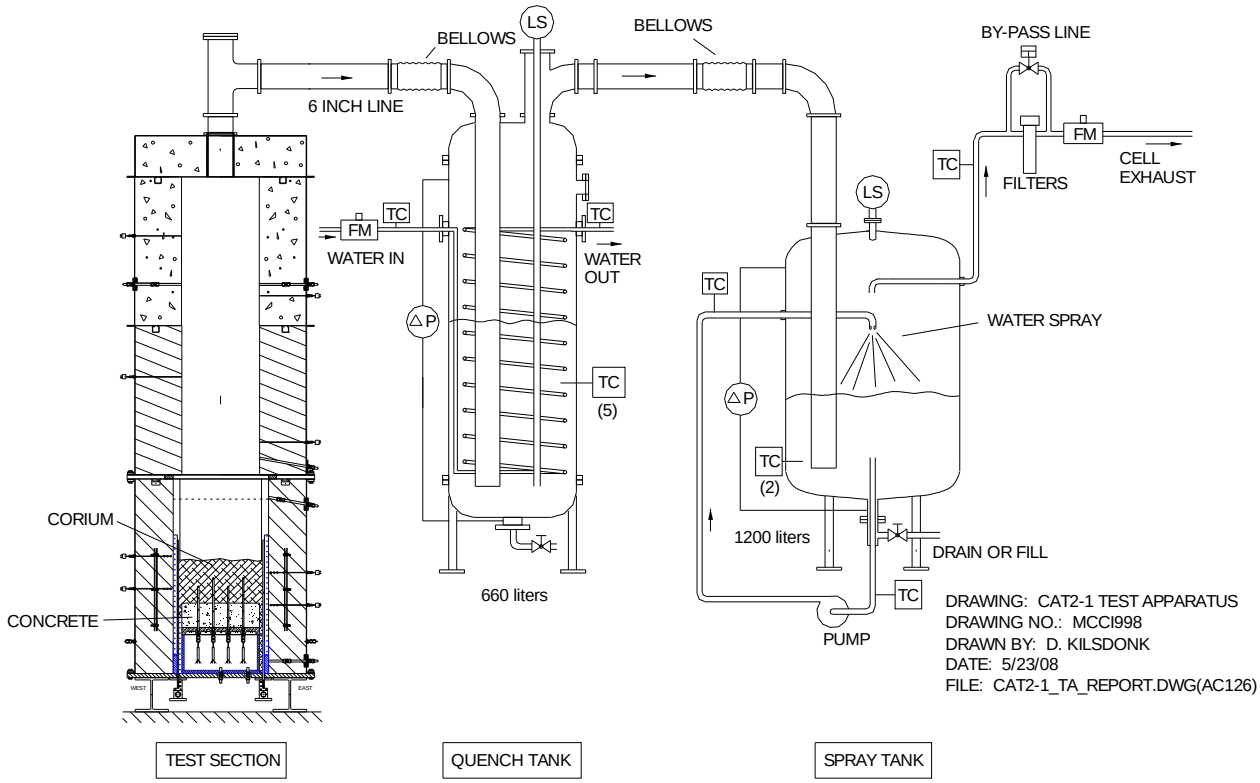

Figure 2-1. Schematic of WCB-1 Test Facility.

The test section for containment of the core melt is located at the bottom of the apparatus. A cross-sectional view showing the water-cooled basemat installation is provided in Figure 2-2. The design utilizes four refractory MgO sidewalls that are each lined with a layer of crushed UO_2

pellets. The pellets serve as an inert (i.e., non-ablative) and highly insulative wall surface. As shown in the figure, the refractory walls are equipped with tungsten backup plates to preclude sidewall melt-through if the pellet layer were to fail and sidewall erosion occurred. The plates are instrumented with contact circuits to alert operating personnel in the control room if melt contacts the plates. This detection/mitigation system forms part of the safety planning for the experiments, and on this basis it would be difficult to modify these components to provide feed throughs for the basemat water lines and instruments. Thus, the connections are brought in through the test section bottom plate. This approach has both design and operational implications, as outlined below.

The refractory sidewalls are contained within a flanged steel form that is used to secure the lower section to the bottom test section support plate and the middle sidewall section. The flanges allow the lower sidewalls to be disassembled to reveal the solidified corium and water-cooled basemat following the test. Aside from the instrumented basemat, multi-junction Type C thermocouple assemblies are cast within the sidewalls so that the time-dependent heat loss from the melt can be calculated from the local temperature gradient and the thermal conductivity of the MgO.

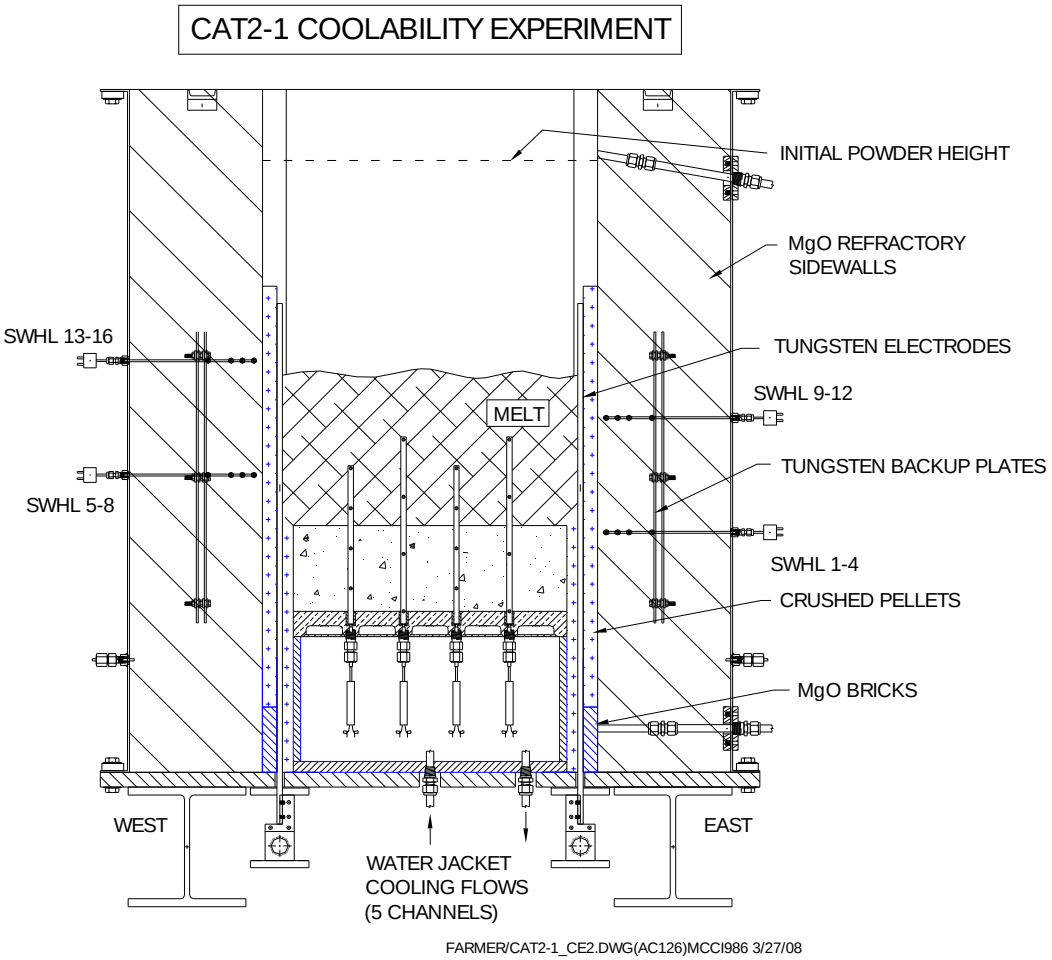

Figure 2-2. Side View of Test Section Showing Water-Cooled Basemat Installation.

Details of the water-cooled basemat design are shown in Figures 2-3 and 2-4. The overall layout consists of a 15 cm deep layer of sacrificial concrete that sits on top of the water-cooled basemat plate. The plate consists of five parallel cooling channels that are machined out of a monolithic piece of 4.4 cm thick Type 304 stainless steel. Although carbon steel would be a more attractive construction material due to the higher thermal conductivity, melting point, and lower material cost, a non-magnetic material must be used to preclude induction heating of the plate by the power supply used to resistively heat the melt. . The basemat is the critical feature in this experiment, and it is essential to preclude spurious system failures that could develop as a result of fabrication techniques that are adopted to reduce costs. Although the monolithic design approach requires a great deal of machining, it is nonetheless adopted to minimize the chance of spurious water leaks that could develop if the plate were manufactured using a cheaper method in which parts are sealed with gaskets, since these interfaces could develop leaks if thermal stresses warped the plate during the test.

In the original design concept for this test presented at the 3rd PRG meeting, the basemat was segmented with non-conductive electrical material (i.e., micarda) so that a shorting path could not develop if melt were to come into direct contact with the steel plate in two different locations. However, there is a concern that the insulation material could cause local hot spot(s) to form that could impede plate thermal performance, and on this basis the segmentation is omitted in this latest design iteration. Thermal analysis provided later in this section indicates that the plate should, under normal operating conditions, be protected by an insulating corium crust, and therefore the technical risk associated with omitting the segmentation is deemed to be small.

As described in Section 2.2, the test assembly is instrumented to measure overlying melt pool temperature, ablation profile of the sacrificial concrete, and the plate/coolant thermal response. The plate instrumentation layout has also been designed to minimize penetration of the water channel that could lead to the development of leaks over the course of the test. For the multi-junction thermocouple assemblies devoted to measuring melt temperature and basemat erosion, this is accomplished by mounting the assembly feed throughs in the unmachined regions between the individual coolant channels (see Figures 2-8 and 2-9 in Section 2.2). This somewhat limits potential locations for the assemblies, but nonetheless ensures that the feed throughs cannot provide a leak path for water. Another design requirement is to electrically isolate these thermocouple assemblies from the basemat to prevent ground loops that would present alternative current paths for the current providing DEH to the melt. This is accomplished by using ceramic-sleeve gland seals (Conax) to mount the thermocouples to the basemat plate. In addition, the tungsten thermowells that protect the melt temperature thermocouple assemblies are electrically isolated with ceramic (fired lavite) sleeves that are used to seat the base of the wells in the plate.

Aside from the thermocouple assemblies, the water channels are also instrumented with *in-situ* high temperature heat flux meters to provide local heat flux measurements. For these units to be effective, they must be installed directly in the cooling channel so there is no choice

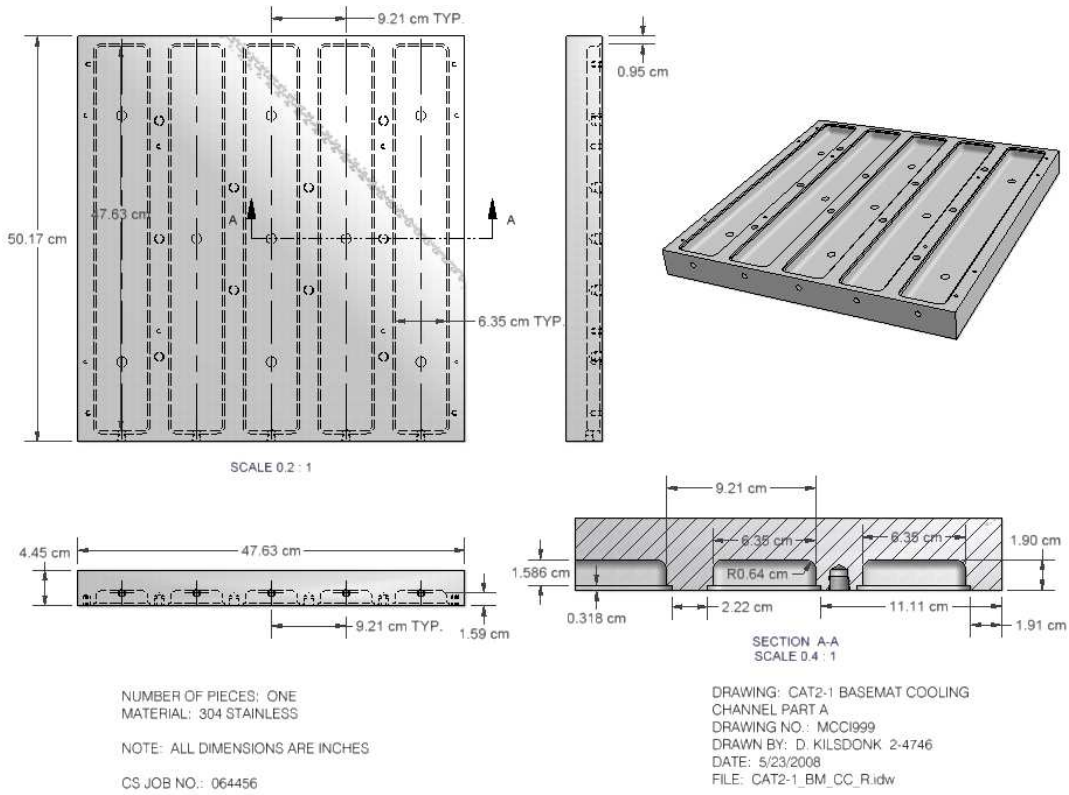

Figure 2-3. Fabrication Details of Water-Cooled Basemat.

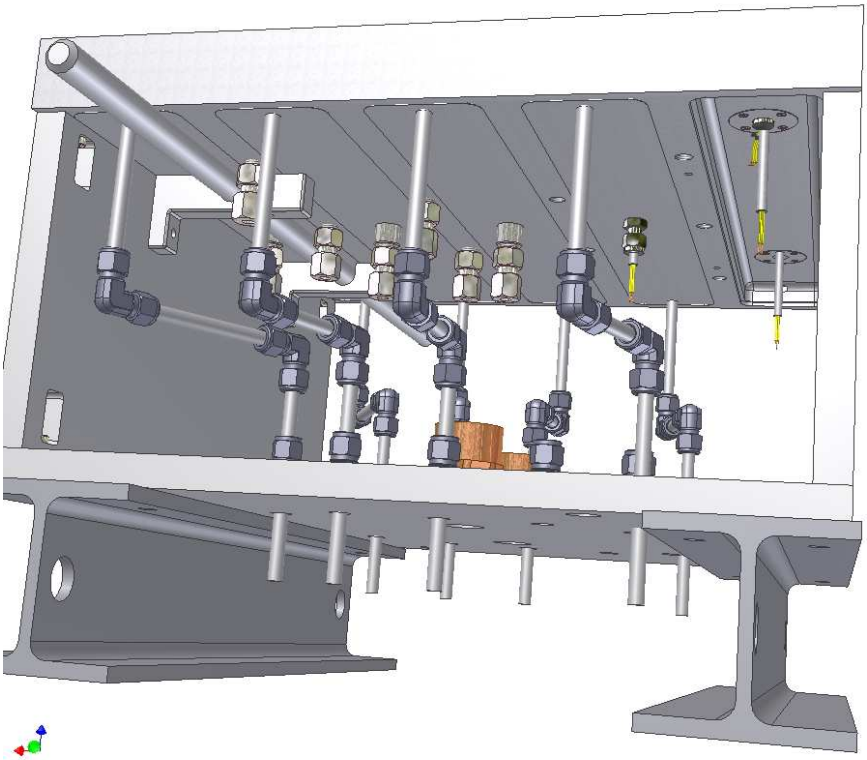

Figure 2-4. Details of Basemat Waterline and Instrumentation Feed Throughs.

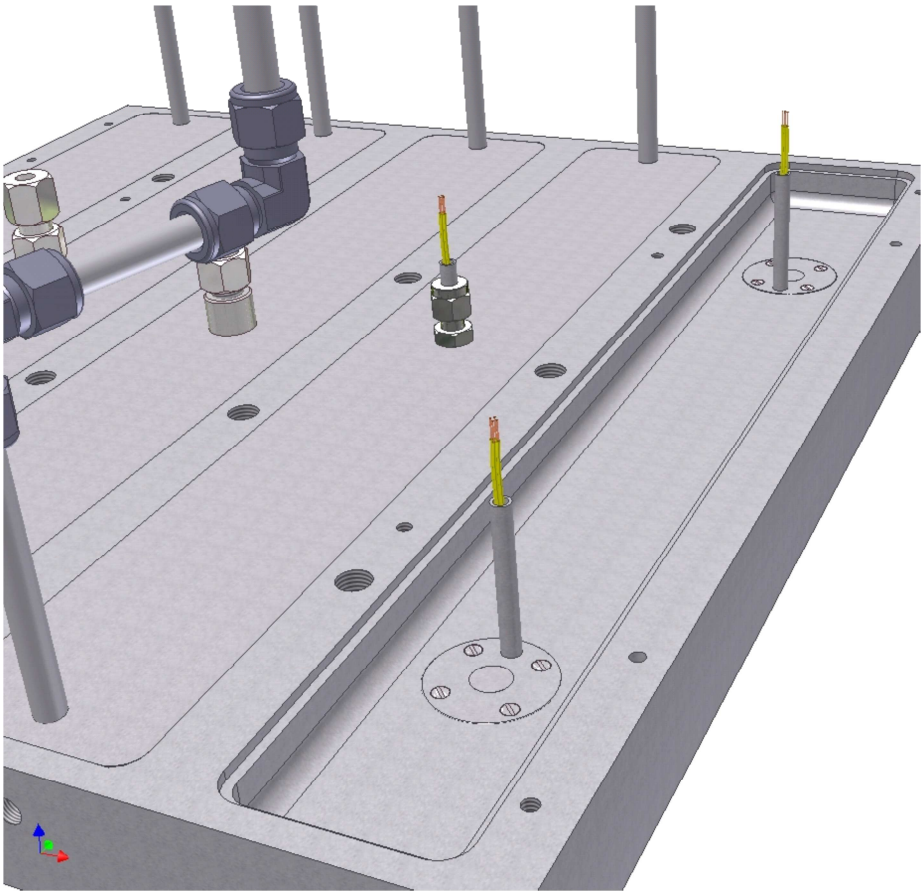

Figure 2-5. Details of Basemat Heat Flux Meter Installation.

but to provide feed throughs that pass through the channel cover plate. To ensure a leak-tight fit, specialty units are utilized that are fitted with a 6.4 mm diameter pipe nipple that passes signal wiring through the channel bottom plate; see Figures 2-4 and 2-5. In this manner, the feed throughs can be sealed using high-grade compression fittings that provide reasonable assurance that the fittings will not develop leaks during the test.

As shown in Figures 2-3 through 2-5, once the heat flux meters are installed, the channels are sealed with 3.2 mm thick 304 stainless steel cover plates that are welded in place to ensure a leak-tight fit.

As noted earlier, the water supply and return lines to the basemat are brought in through the test section base support plate. As shown in Figure 2-6, each channel is equipped with an independent water measurement and control system that includes entrance and exit isolation valves, flowmeter, and a motorized ball valve on the exit side of the plate that allows flow to each channel to be independently adjusted from the control room. Temperature rise across the channel is measured using Type K thermocouples. The channel piping is constructed from 1.3 cm diameter tubing. The individual channel flowrate and water temperature rise data allow the average heat flux to each channel to be calculated. The channels are fed from a 2.5 cm diameter header manifold, and vented through a manifold of the same diameter. The bulk temperature rise across the two manifolds and total mass flowrate allow the average heat flux to the plate to be

calculated for comparison to the local channel measurements determined by the heat flux meters and the individual channel mass flux/temperature rise measurements.

Since the basemat water inlet and exits are from the bottom of the plate, this test cannot investigate situations in which the bulk water outlet temperature approaches saturation, otherwise the channels may vapor-lock and cause premature test termination. Finally, given this design, it is important to vent the air out of the lines before the test section is fully assembled. As shown in Figure 2-6, each channel is equipped with a small (6.4 mm diameter) pipe plug that is mounted at the top of the channel on the inlet side. Prior to installing the test section sidewalls, the water lines will be pressurized and the plugs loosened until all the air is vented and the plugs resealed. After this point, test procedures will not allow the water line return side isolation valves to be opened unless the inlet valves are opened and the lines pressurized. This will prevent air from reentering the system.

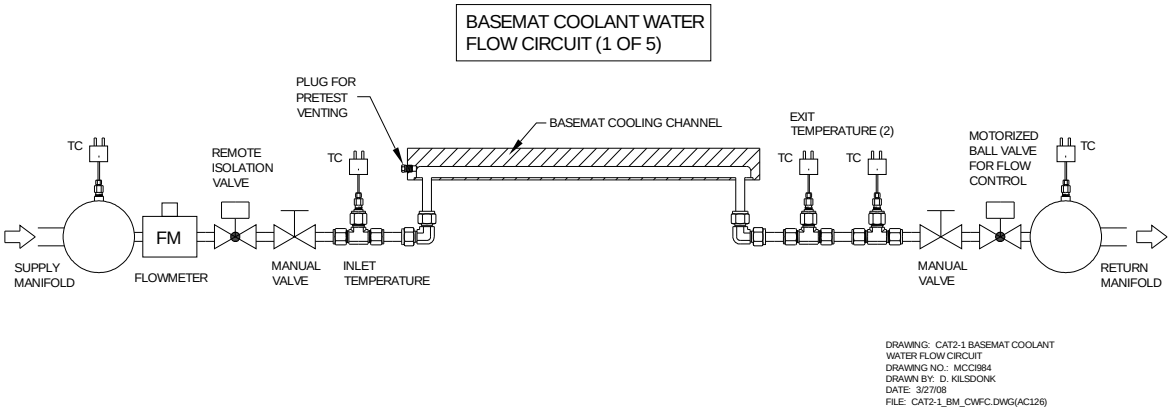

Figure 2-6. Basemat Water Channel Cooling Circuit (1 of 5).

A few simple heat transfer calculations have been performed in order to quantify the cooling plate performance characteristics. The purpose of these calculations is to verify that the cooling circuits are capable of keeping the cooling plate temperature well below its melting temperature. In order to fulfill this purpose, the cooling system must dissipate enough power to maintain a crust between the cooling plate and melt. Two design specifications are imposed to achieve this goal:

1. The heat load for the system is based on previously observed heat fluxes to the concrete sidewalls and basemat. These heat fluxes are typically ~150 kW/m^2.
2. The cooling circuits are to be sized so that they prevent saturated nucleate boiling from occurring anywhere along the channel. A transition from subcooled to saturated boiling is expected to degrade heat transfer in this particular geometry. Flow rates and coolant temperatures are to be selected to ensure that only subcooled boiling may occur.

Thermophysical property data used in the analysis are provided in Table 2-1, while results are shown in Table 2-2. As shown in Table 1-1, the design basis heat flux to the plate is 150 kW/m^2, which corresponds to ~ 7.5 kW to each channel given the channel dimensions (see Figure 2-3). The channel flowrate is selected to maintain a significant bulk subcooling at the design basis heat flux. Thus, the channel volumetric flowrate is chosen as 12 liters/min per

channel, which yields a bulk temperature rise of ~ 9 ºC per channel. Given the channel dimensions and flowrate, the channel hydraulic radius and Reynolds number are found to be 2.54 cm and 8890, respectively. The heat transfer coefficient is evaluated from the well-known Dittus Boelter correlation; i.e.,

$$h = \begin{cases} 7.6\dfrac{k}{D_h}; & \mathrm{Re} < 2300 \\ 0.024\,\mathrm{Re}^{0.8}\,\mathrm{Pr}^{0.4}\left(\dfrac{k}{D_h}\right); & \mathrm{Re} \geq 2300 \end{cases}.$$

The flow is turbulent (i.e., Re > 2300), and the convective heat transfer coefficient is thus evaluated from the second expression given above as 1405 W/m^2-ºC.

Table 2-1. Thermophysical Properties Assumed in the Analysis.

Property	Water	304 Stainless	Corium Crust
Density (kg/m^3)	990	8000	5000
Thermal conductivity (W/m-ºC)	0.64	14	2
Specific heat (J/kg-ºC)	4178	500	600
Freezing temperature (ºC)	N/A	N/A	1130
Viscosity ((kg/m-s)	$5.6 \cdot 10^{-4}$	N/A	N/A

Table 2-2. Channel Thermal Analysis at Design Basis Conditions (150 kW/m^2 heat flux to plate, 12 liters/minute water flowrate per channel).

Parameter	Value
Plate thickness over flow channels (cm)	2.54
Channel cross-sectional flow area (cm x cm)	1.59 x 6.35
Channel planar area exposed to melt pool (cm x cm)	10 x 50
Channel hydraulic diameter (cm)	2.54
Channel design water flowrate (cm^3/s)	200
Channel water flow velocity (cm/s)	19.8
Channel inlet water temperature (ºC)	15
Plate design basis heat flux from melt pool (kW/m^2)	150
Channel Reynolds No. (-)	8890
Channel heat transfer coefficient (W/m^2-ºC)	1405
Individual channel thermal loading from melt pool (kW)	7.5
Bulk water temperature rise along channel (ºC)	9.0
Channel water outlet temperature (ºC)	24.0
Water film temperature rise to plate assuming single-phase convection (ºC)	106.7[a]
Channel plate inner surface temperature (ºC)	~ 100
Temperature rise across plate (ºC)	272
Exterior surface temperature of plate beneath crust (ºC)	372
Crust temperature gradient (T_f - T_i)	758
Corresponding crust thickness to balance thermal load (mm)	10

[a]The channel inner surface temperature is calculated to slightly exceed saturation, while the bulk temperature at the channel outlet remains highly subcooled. Thus, subcooled boiling will occur on the channel inner surface that will maintain the surface temperature near saturation.

With this information and the design heat flux, the water film temperature rise between the bulk and channel surface is evaluated as ~ 107 ºC. Thus, the wall surface temperature required to dissipate the heat under single phase flow conditions is above saturation, and as a

result, subcooled nucleate boiling on the bottom of the plate will develop, albeit at a low level given the low overall water temperature rise across the channel. In any event, onset of subcooled boiling will significantly increase the heat transfer coefficient, thereby maintaining the channel inner surface temperature near saturation. Assuming this boundary condition, then the conduction-limited temperature rise across the plate required to dissipate the design basis heat flux is 272 ºC, and the plate exterior surface temperature will be ~ 373 ºC. Assuming a corium crust forms on the plate, then the temperature rise across the crust will be ~ 758 ºC assuming the crust surface is maintained at the corium solidus temperature, which is further assumed to equal the siliceous concrete solidus of ~ 1130 ºC [1]. With this data and an assumed crust thermal conductivity of ~ 2 W/m-ºC, the equilibrium crust depth that will form on the plate is calculated as ~ 1 cm.

To summarize, after the system equilibrates at the design heat flux, the water channels should exhibit an average temperature rise of ~ 9 ºC, with the boundary condition on the plate inner surface being highly subcooled nucleate boiling. The exterior temperature of the plate should come to equilibrium at ~ 373 ºC, with the plate surface protected by a ~ 1 cm deep corium crust. This of course assumes that the concrete is fully eroded, and the corium immediately forms a crust on the relatively cold steel plate. However, the situation will not differ significantly if a slag crust forms on the surface, since the thermal conductivities of these two media are approximately the same.

Returning to the balance of the apparatus design description, the melt is produced through an exothermic chemical reaction yielding the target mass over a timescale of ~ 30 seconds. After the chemical reaction, DEH simulating decay heat is applied through two banks of tungsten electrodes. As shown in Figures 2-2 and 2-3, the electrodes line the interior surfaces of the two opposing MgO sidewalls. The electrodes are 9.5 cm in diameter and aligned in a row with a pitch of 1.9 cm. They are attached by copper clamps and water-cooled buss bars to a 560 kW AC power supply.

A few minutes after the melt is formed, ablation of the sacrificial concrete basemat will commence. As shown in Figure 2-1, a large (15 cm diameter) gas line is used to vent the helium cover gas and the various gas species arising from the core-concrete interaction (i.e., CO, CO_2, H_2O, and H_2) into two adjacent tanks that are partially filled with water. In the initial phase of the experiment as the concrete is eroded, the tanks serve to cool the off-gases and filter aerosols generated from the core-concrete interaction. In the late phase after the cavity is flooded, the tanks serve to condense the steam and, based on the measured condensation rate, provide data on the corium cooling rate. In either case, the helium covergas and non-condensables (CO, CO_2, and H_2) pass through the tanks and are vented through an off gas system that includes a demister, filters, and a gas flow meter. The gases are eventually exhausted through the containment ventilation system and a series of high efficiency filters before finally being released from the building stack.

After a specified period of interaction, the cavity will be flooded using an instrumented water supply system. The water enters the test section through two weirs located in the opposing (non-electrode) sidewalls of the top test section. The water flows down the test section interior walls and then atop the core melt. The water supply system is shown in Figure 2-7.

2.2 Instrumentation and Data Acquisition

The WCB-1 facility is instrumented to monitor and guide experiment operation and to log data for evaluation of the lateral and axial erosion rates. Principal parameters that are monitored during the course of the test include the power supply voltage, current, and gross input power to the melt; melt temperature and temperatures within the concrete basemat, sidewalls, and water-cooled basemat; supply water flow rate to the basemat and to the test section; water volume and temperature within the test apparatus, and water volume and temperature within the quench system tanks. Other key data recorded by the DAS includes temperatures within test section structural sidewalls, melt/crust upper surface temperature, off gas temperature and flow rate, and pressures at various locations within the system.

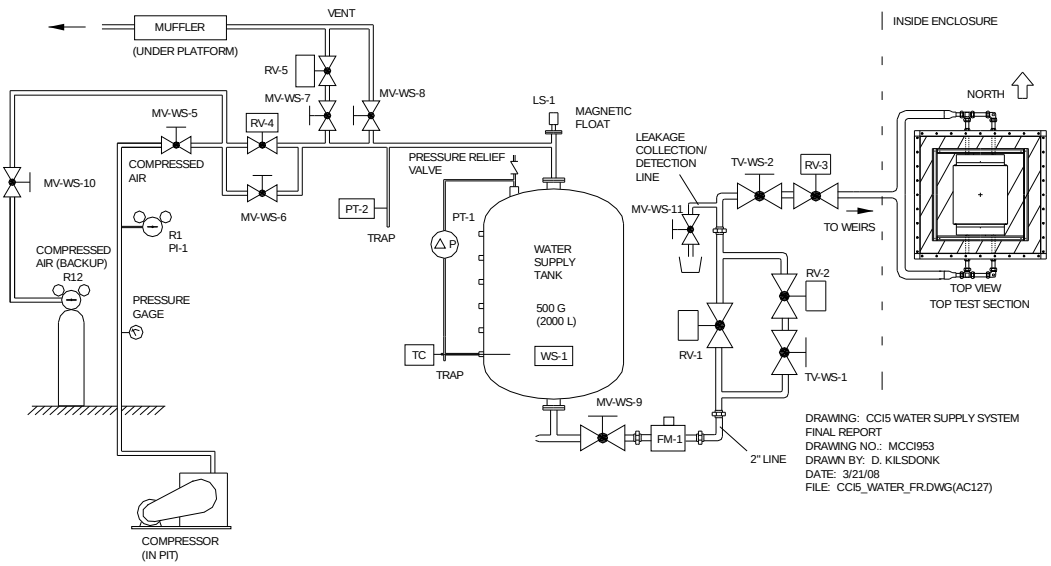

Figure 2-7. Test Section Water Supply System.

Detailed plan and elevation views of the basemat thermocouple layout are provided in Figures 2-8 and 2-9, respectively. The basemat is instrumented to monitor melt temperature during both the concrete ablation and plate-cooling phases of the test using multi-junction Type C thermocouples in tungsten thermowells, and also to track concrete ablation during the early sacrificial erosion phase using multi-junction Type K thermocouples cast directly into the basemat. The water-cooled basemat and basemat water supply system are instrumented to provide local and global heat transfer performance data.

Other significant test instrumentation includes a stationary (lid mounted) video camera for observing physical characteristics of the interaction. In addition, a pyrometer is used to measure the debris upper surface temperature during periods in which aerosol production does not optically occlude the view of the surface

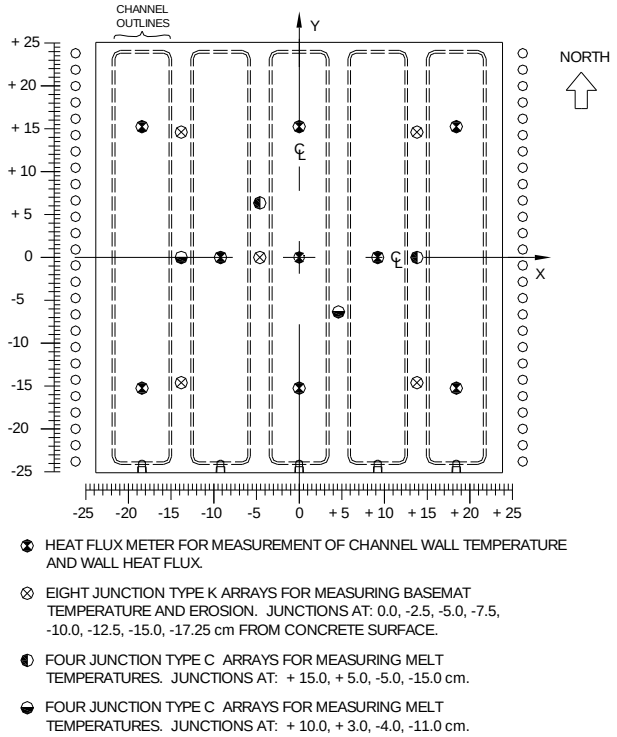

Figure 2-8. Plan View of Basemat Instrumentation Layout (dimensions are in cm).

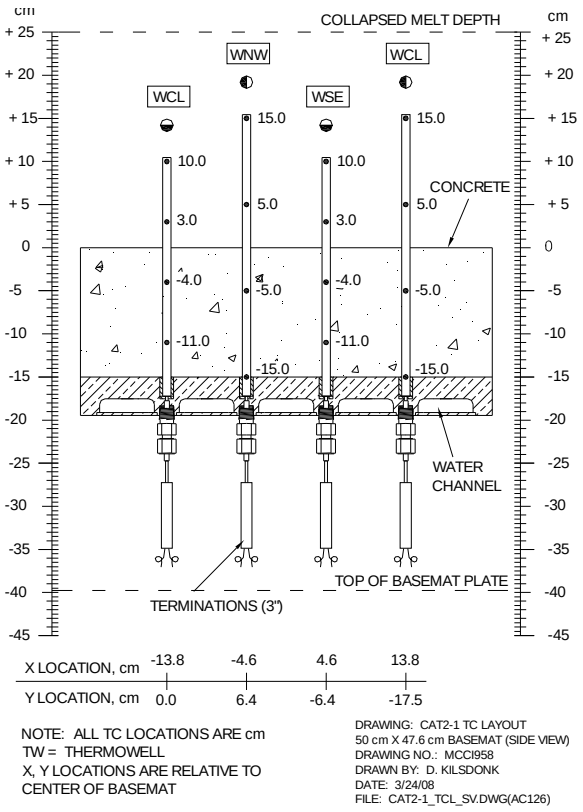

Figure 2-9. Elevation View of Basemat Type C Thermocouple Locations.

All data acquisition and process control tasks are managed by a PC executing LabVIEW 6.i under Windows XP. Sensor output terminals are connected inside the test cell to model HP E1345A 16-channel multiplexers, which are integrated into a mainframe chassis in groups of eight. An illustration of the DAS setup is provided in Figure 2-10. The multiplexers direct signals to an HP E1326B 5 ½ digit multimeter incorporated into each chassis. Three independent 128 channel systems are used for a total capacity of 384 channels.

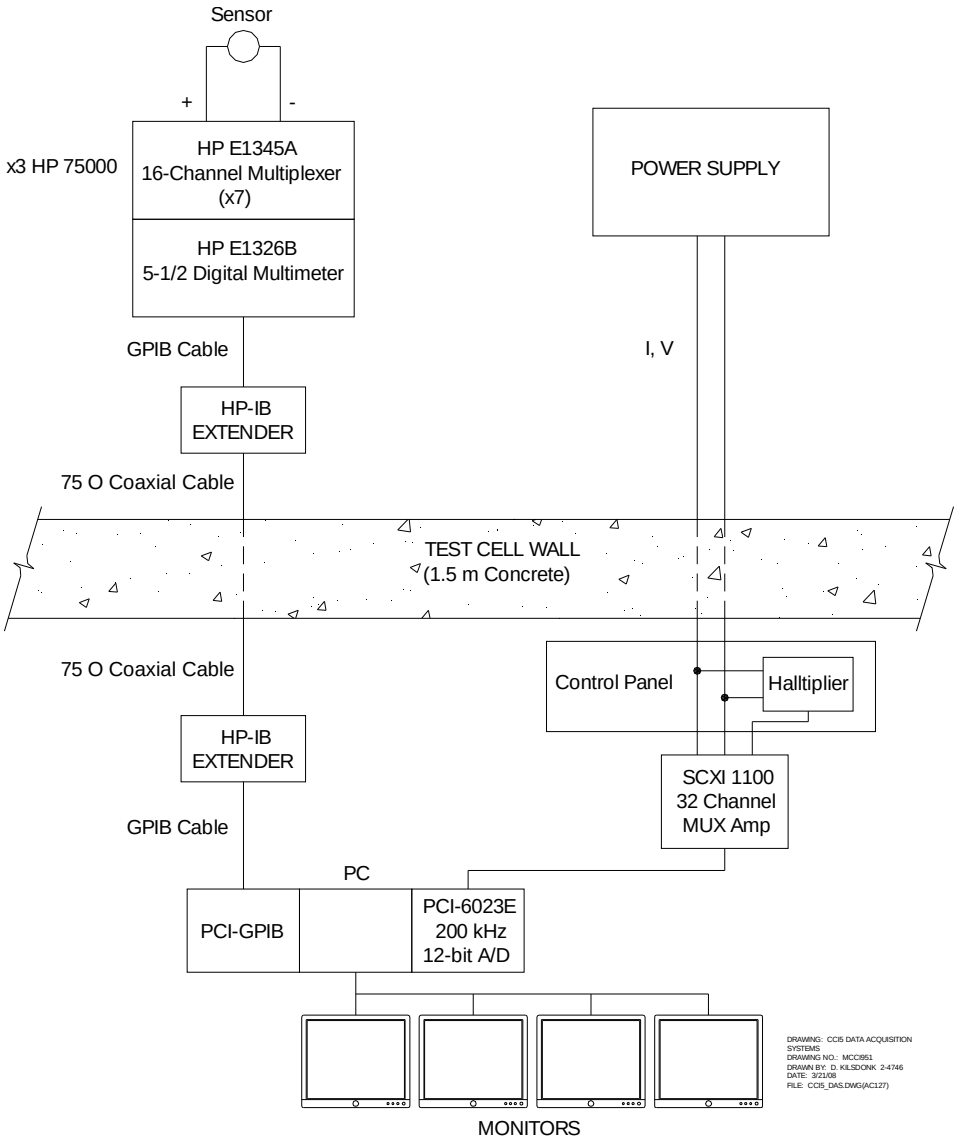

Figure 2-10. WCB Data Acquisition and Control Systems.

Signal noise is reduced by the digitizer through integration over a single power line cycle (16.7 ms). The digitized sensor readings are routed from the test cell to the PC in the control room via two HP-IB extenders. The extenders allow the ASCII data from the HP to be sent through the cell wall over a BNC cable. The extender within the control room then

communicates with a GPIB card within the PC. This configuration also permits remote control of the multimeter through LabVIEW.

Integration of the signal over the period of a power line cycle limits the speed with which the multiplexer can scan the channel list. The minimum time for the digitizer to scan the channel list is ~1.7 s (16.7 ms • 100 channels/chassis for this test). Though the three systems operate independently, implying the ability to update all 300 channels in roughly two seconds, the actual time required for the update is about 5.5 s.

2.3 Corium Composition

As shown in Table 1-1, the corium composition for WCB-1 is specified to contain 8 wt % calcined siliceous concrete as an initial constituent. As part of the developmental work for the CCI-1 experiment [2], a specific thermite was developed to produce this particular melt composition. The thermite reaction is of the form:

$$1.22U_3O_8 + 3.3Zr + 0.58Si + 1.14SiO_2 + 0.026Mg + 0.36\ CaO + 0.12Al + 1.842CrO_3 \rightarrow$$

$$3.66UO_2 + 3.3ZrO_2 + 1.72SiO_2 + 0.026MgO + 0.91CaO + 0.36Al_2O_3 + 1.842Cr;$$

$$Q = -252.2\ \text{kJ/mole}\ (1.71\ \text{MJ/kg});$$

$$T_{adiabatic} = 2572\ °C$$

$$T_{actual} \sim 2100\ °C$$

The bulk composition of the melt produced from this reaction is summarized in Table 2-3, while the detailed pre- and post-reaction compositions are provided in Table 2-4. Note that the pre- and post-reaction compositions shown in these tables do not include the mass of the UO_2 pellets that are used to line the test section MgO sidewalls; see Figure 2-2. This material does not participate in the initial exothermic chemical reaction, and remains essentially intact as a protective layer during the ensuing test sequence. The actual mass of UO_2 that dissolves into the melt over the course of the experiment will be determined as part of the posttest examination activities.

The 400 kg thermite charge is packed into the test section in a large, 1.7 mil aluminized Saran bag which is pre-installed over the basemat. The thermite is packed in the bag to prevent water absorption by CrO_3 and concrete oxides (principally CaO and SiO_2), since these constituents are hygroscopic.

2.4 Concrete Composition

The composition of the WCB-1 concrete is tentatively specified to be of the siliceous type. For the purposes of pretest planning, the specific composition is chosen to be the same as that used in the CCI-3 experiment [2], since materials for fabrication of this concrete type are currently in stock at ANL. The engineering composition for this particular concrete is shown in Table 2-5. The sand and aggregate for the mix were supplied by CEA as an in-kind contribution to the program. The estimated chemical composition for this concrete is provided in Table 2-6.

This composition is based on analysis of a specimen taken from the CCI-3 concrete archive sample [2]. The actual composition of the concrete for Test WCB-1 will be determined through chemical analysis of a specimen that will be collected during fabrication of the basemat component.

Table 2-3. Post-Reaction Bulk Composition for WCB-1 Thermite.

Constituent	Wt%
UO_2	60.97
ZrO_2	25.04
Calcined Concrete	8.08[b]
Cr	5.91

[b]Calcined siliceous concrete: 79.0/0.9/15.4/4.7 wt% SiO_2/MgO/CaO/Al_2O_3

Table 2-4. Detailed Pre- and Post-Reaction Compositions for WCB-1 Thermite.

Constituent	Reactant		Product	
	Wt%	Mass (kg)	Wt%	Mass (kg)
U_3O_8	63.38	253.52	-	-
UO_2	-	-	60.97	243.88
Zr	18.53	74.12	-	-
ZrO_2	-		25.04	100.16
Si	1.00	4.00	-	-
SiO_2	4.23	16.92	6.38	25.52
Mg	0.04	0.16	-	-
MgO	-	-	0.07	0.28
Al	0.20	0.80	-	-
Al_2O_3	-	-	0.38	1.52
CaO	1.25	5.00	1.25	5.00
CrO_3	11.37	45.48	-	-
Cr	-	-	5.91	23.64
Total	100.00	400.00	100.00	400.00

Table 2-5. Engineering Composition of WCB-1 Siliceous Concrete Basemat.

Constituent	wt %	Size Distribution
Aggregate	47.4	5-8 mm: 16.6 wt % 8-11 mm: 20.4 wt% 11-16 mm: 10.4 wt%
Sand	30.6	0-2 mm: 12.2 wt % 2-4 mm: 18.4 wt %
Type 1 Cement	15.3	N/A
Tap Water	6.7	N/A

3.0 TEST PROCEDURES

3.1 Pretest Preparations

Assembly of the apparatus begins through the installation of tungsten electrodes into machined copper electrode clamps. The electrode clamps are then attached to the bottom of the 1.9 cm thick aluminum support plate, which serves as the foundation for the entire apparatus. With the electrode clamps installed, the support plate is moved into position on the test stand. The water-cooled basemat is then installed, plumbed up to the supply and return water manifolds, vented of air, and then thoroughly leak checked. Once these steps are completed, the four sidewalls are then set in place on the support plate. The lower section flange bolts and clamping bars are then installed and tightened. Following this step, the basemat instruments are connected to terminal boxes that are prewired to the data acquisition system.

Table 2-6. Chemical Composition of Siliceous Concrete (CCI-3 basis [2]).

Constituent	Wt %
SiO_2	60.99
CaO	17.09
Al_2O_3	3.61
Fe_2O_3	1.52
MgO	0.87
MnO	0.04
SrO	0.04
TiO_2	0.16
SO_3	0.44
Na_2O	0.67
K_2O	0.83
CO_2	9.98
H_2O	3.76[a]

[a]Free water content is 2.33 wt % while bound water content is 1.43 wt %.

Once the lower section is assembled, preparations for loading of the corium charge are initiated. A single large 1.7 mil aluminized Saran bag is preinstalled over the basemat. During loading, the thermite is repackaged into this bag to reduce the amount of bagging material present in the thermite charge. Once the large bag is filled with thermite, the sparklers used to initiate the chemical reaction are placed in the top of the powders, and the bag is folded and sealed.

Once loading is completed, the remainder of the test apparatus is assembled. This includes installation of the two upper sections and the enclosure lid. Peripheral instruments are then installed and connected to terminal boxes. The main gas line from the test section to the quench tank is installed, as well as the pressure relief line from the test section to the auxiliary tank. After assembly is completed, system checkout is performed to ensure that the facility is in proper working order. This includes a proof test of the test section at 83 kPad, which is 20 % in excess of the pressure relief system activation pressure of 69 kPad.

3.2 Test Operations

Prior to initiating the thermite reaction, a helium gas flow rate is established through the lid of the test section. Coolant water flow to the basemat is also initiated at this time. The thermite is ignited using the sparklers located at the top of the powder charge. Once the reaction is complete (~ 30 seconds), the power supply is ramped at a rate of ~ 3000 Amps/minute up to the initial target power level. As shown in Table 1-1, initial target power for the core-concrete interaction phase is 80 kW. After melt formation, the input power would be held constant at the 80 kW level until the concrete is eroded to a depth of 12.5 cm, as evidenced by thermocouple readings near the bottom of the concrete.

Once the concrete ablation depth reaches 12.5 cm, leaving a concrete layer 2.5 cm thick over the water-cooled basemat, the cavity will be flooded and the input power will be held constant at the 80 kW level until the system comes to thermal equilibrium. The determinants for thermal equilibrium are that the steaming rate from the test section, as well as the melt and water channel exit temperatures, remain stable for 15 minutes.

Following this initial stage of operations with water present in the cavity, there will not be any melt pool gas sparging from concrete decomposition gases since the concrete will eventually be fully eroded. As a result, the test conditions will somewhat resemble a SSWICS water ingression test, but with a water-cooled basemat and with input power into the melt by direct electrical heating. Thus, the recommended power supply operating procedure is constant voltage so that if water does ingress into the material, then the input power should decrease at a relatively constant rate as the material is quenched. However, if the power does not fall appreciably, then the conclusion is that the input power lies above the dryout limit. If this situation occurs, then the input power could be reduced in 10 kW intervals spaced out at ~ 15 minute intervals until the power does begin to decrease at constant voltage. This will define the dryout limit for the melt mixture, which would be another important data point to add to the SSWICS water ingression database. However, this measurement would be unique since it would be determined with input power into the melt, which more closely simulates prototypic conditions. The test would be terminated on the basis of temperature measurements in the bottom of the melt pool approaching saturation conditions.

3.3 Posttest Operations

Following the experiment, the apparatus will be carefully disassembled to document the posttest debris configuration. The test section main gas line, lid, and the top and middle sidewall sections are removed to reveal the lower test section, which contains the solidified core debris. The upper surface of the debris will then be photographed, and a few specimens collected for chemical analysis.

After this information is collected, the four MgO sidewalls of the lower test section will be removed, thereby fully revealing the solidified corium over the basemat plate. Once the corium is revealed, the material will be extensively photographed and additional samples collected for chemical analysis. Measurements will be taken to document key dimensions and features. When these measurements are completed, an attempt will be made to remove the

corium from the basemat plate so that the plate can be examined for signs of damage or interaction with the corium. The material will then be packaged and archived as part of the test records. The MgO sidewall sections will be cleaned for reuse in subsequent tests.

4.0 REFERENCES

1. D. H. Thompson, M. T. Farmer, J. K. Fink, D. R. Armstrong, and B. W. Spencer, "ACE Phase C Final Report: Volume I-MCCI Thermalhydraulic Results," EPRI/ACE-TR-C42, September, 1997

2. M. T. Farmer, S. Lomperski, D. J. Kilsdonk, and R. W. Aeschlimann, "OECD MCCI Project 2-D Core Concrete Interaction (CCI) Tests: Final Report," OECD/MCCI-2005-TR05, January 2, 2006.